Halogen Precursor Route to Poly[(2,3-diphenyl-*p*-phenylene)vinylene] (DP-PPV): Synthesis, Photoluminescence, Electroluminescence, and Photoconductivity

Wai Chou Wan,[#,†] Homer Antoniadis,[†,⊥] V. E. Choong,[‡] H. Razafitrimo,[‡] Y. Gao,[‡] William A. Feld,[§] and Bing R. Hsieh*[,†,#]

Center for Photoinduced Charge-Transfer and Department of Physics and Astronomy, University of Rochester, Rochester, New York 14627, Xerox Corporation, 800 Phillips Road, 114-39D, Webster, New York 14580, and Department of Chemistry, Wright State University, Dayton, Ohio 45435

Received July 10, 1997[⊗]

ABSTRACT: Thin films of poly[(2,3-diphenyl-*p*-phenylene)vinylene] (DP-PPV) have been prepared via a chlorine precursor route (CPR). This involves the polymerization of 1,4-bis(chloromethyl)-2,3-diphenylbenzene with 1.0 equiv of potassium *tert*-butoxide to give the chlorine precursor polymer of DP-PPV. The chlorine precursor was thermally converted at different temperatures to give DP-PPV with different degrees of conversion. The conversion process was monitored by in situ photoluminescent (PL) spectroscopy. The onset of conversion was about 150 °C, and full conversion could be achieved at 170−250 °C. The degree of conversion was a function of the heating temperature rather than the duration of heating. The fully converted DP-PPV showed lower photoconductivity and higher PL intensity than PPV. Although partially converted DP-PPV showed bright PL, we have not been able to observe its EL. The electroluminescence (EL) of the single layer ITO/DP-PPV/Mg and the bilayer ITO/DP-PPV/Alq_3/Mg LED devices is also reported. A significant improvement in the quantum efficiency (up to 0.7% ph/el) and a reduction in the turn-on voltage of the device were found upon incorporation of the Alq_3 layer. These observations suggest that Alq_3 enhances the injection of electrons and also participates in the recombination process.

Introduction

The discovery of electroluminescence (EL) in poly (*p*-phenylenevinylene) (PPV)[1] has stimulated a great deal of interest in conjugated polymers and oligomers for solid state semiconductor device applications[2−4] such as photovoltaic cells,[5,6] xerographic photoconductors,[7] field effect transistors,[8−11] light-emitting diodes (LED),[12] and light-emitting electrochemical cells.[13,14] PPV derived from the sulfonium precursor route (SPR) can be processed in many different ways to give PPV thin films with different luminescence characteristics.[12,15] Enhancement of light-emitting efficiency and tuning of the color have been achieved.[12,15] The approaches used for varying the luminescence properties of PPV include control of the conjugation length and side groups and modifications in processing for PPV.[2,3,12,15]

The overall synthetic methodology for the preparation of PPV thin films can be divided into three main categories: (1) side chain derivatization, (2) precursor approach, and (3) in situ polymerization. We have focused on the first two methods and have prepared PPV and a wide range of PPV derivatives.[2,16−20] Three precursor routes, namely the sulfonium precursor route (SPR),[1,2] the halogen precursor route (HPR),[2,17] and the xanthate precursor route (XPR),[21] have been used for the fabrication of PPV LEDs. The three routes rely on the preparation of a soluble precursor polymer that is then cast into thin films and converted to the final conjugated PPV films through heating. These three precursor routes are highly complementary to each other and have led to the synthesis of a wide range of PPV derivatives. Because of various synthetic difficulties, the SPR approach is limited and is useful mainly for the preparation of PPV.[2,17−20] However, the water soluble polyionic sulfonium precursor polymer has enabled a unique opportunity for the fabrication of heterostructural LEDs via a self-assembly process.[22,23] In general, XPR is useful for the preparation of PPV and those PPV derivatives with small side groups such as methyl and methoxy groups.[21] The chlorine precursor route (CPR), one of many HPRs, is useful for the preparation of PPV with relatively large side groups such as phenyl, phenoxy, and hexyloxy.[24]

We have focused our research on the fabrication of PPV-based LEDs via CPR.[17−20] This effort has led to the recent communication of the fabrication of poly[(2,3-diphenyl-*p*-phenylene)vinylene] (DP-PPV) LED.[18] We report here the synthesis and photophysical properties of DP-PPV synthesized via the CPR route. The conversion process of the soluble precursor polymer to DP-PPV thin films was studied by absorption and photoluminescence (PL) spectroscopies. The onset of conversion occurred at 150 °C, and a full conversion could be achieved at 170−250 °C. Fully converted DP-PPV has better electroluminescence and photoluminescence properties but lower photoconductivity relative to PPV. We have also demonstrated that by incorporating an electron transport layer to the DP-PPV LED device we can enhance the efficiency of EL.

Experimental Section

General Methods. All chemical reagents used were purchased from Aldrich. All organic solvents were used without any further purification. Distilled water was used in the reactions, and aqueous NaOH was freshly prepared for each reaction. ^{1}H NMR spectra were measured with a Bruker 360

[#] Center for Photoinduced Charge-Transfer, University of Rochester.
[†] Xerox Corp.
[‡] Department of Physics and Astronomy, University of Rochester.
[§] Wright State University.
[⊥] Present address: Hewlett-Packard Labs, 3500 Deer Creek Rd., 26M-7, Palo Alto, CA.
[⊗] Abstract published in *Advance ACS Abstracts,* October 1, 1997.

S0024-9297(97)01025-5 CCC: $14.00

MHz spectrometer. Elemental analyses were performed by Galbraith Laboratories Inc. Melting points were measured using a Haake Buchler melting point apparatus and are uncorrected. GPC were measured on a Waters Modular system with a photodiode array and 410 refractive index. A 1% THF solution of the precursor polymer with THF as the eluent and polystyrene standard was used. Infrared measurements were made on a Perkin-Elmer 1750 FTIR.

Thin polymer films for optical absorption and photoluminescence were prepared by spin casting of a 1 wt % toluene solution of the precursor polymer onto a glass substrate, yielding a polymer film approximately 400 Å thick. Each sample was heated at a preselected temperature under a flow of dry nitrogen for 2 h. The samples were stored under low vacuum. Photophysical measurements were made at room temperature, in air or under an argon atmosphere. UV−visible spectra were obtained on a Perkin-Elmer Lambda 9 spectrophotometer. Steady state PL measurements were done on a Spex Fluorolog-2 fluorometer equipped with a DM3000F spectroscopy computer, where the samples were positioned such that the emission was detected at 22.5° from the incident beam. PL was also monitored from the conversion chamber with a Photo-Research SpectraScan 650 photocalorimeter. The emission spectra were obtained at 380 nm with an excitation power of 1 mW/cm^2.

Time-resolved PL decay measurements were performed using time-correlated single photon counting. The excitation system consisted of a mode-locked frequency-doubled Nd:YAG laser (Quantronix Model 416) synchronously pumping a cavity-dumped dye laser (Coherent model 703D) circulating rhodamine 6G. The dye laser pulses were typically 10 ps in duration at a repetition rate of 38 MHz with an excitation wavelength of 380 nm. The time-resolved emission spectra were taken under different storage and measurement conditions to study the effects of air exposure on the samples. The spectra are normalized to the same height for visual clarity. Samples were stored under low vacuum or in air after conversion, and sample measurements were also performed in air or under continuous nitrogen flow.

A free-standing DP-PPV film was prepared for photoconductivity measurement as follows: About 2.0 mL of a 2.0 wt % chlorine precursor polymer in toluene was transferred onto a leveled 2.0 in. × 2.0 in. glass substrate and then covered with a Petri dish to allow slow solvent evaporation. The dried film was then converted at 200−250 °C for 2 h under an argon atmosphere. Upon cooling, the film was lifted from the substrate with dry ice. Two aluminum contacts were deposited onto opposite sides of the film by vacuum deposition. The samples were mounted in an electrically shielded box and in some instances in a vacuum chamber. Illumination was in the applied field direction. The light source used was a xenon lamp dispersed by a holographic grating monochromator broadcasting into an optical fiber bundle. A computer-controlled stepper motor was employed for wavelength dependence studies. A series of neutral density filters were used to regulate the light intensity. Current vs voltage characteristics were measured using an electrometer and a digital power supply under computer control. The spectra shown are presented without correction due to losses caused by the electrodes.

EL emission spectra were performed on an Oriel InstaSpec IV CCD system equipped with a imaging monochromator model Oriel MS127i. An optical fiber was used to couple the EL light to the monochromator. The output of the CCD array was stored and processed by a personal computer. The emission PL and EL spectra shown in this paper have not been corrected for possible distortions due to monochromators. The luminance−current−voltage measurements were performed by using an HP 4155A Semiconductor Parameter Analyzer. A silicon photodiode (area 1 cm^2) was placed in front of the EL device and used for both the efficiency and luminance measurements. Two different calibrations were used: one estimated the external quantum efficiency by using an integrating sphere, and the other estimated the luminance by using a photometer aimed directly at the emitting area. The electrical and optical measurements presented here were performed under dry nitrogen and ambient conditions, respectively.

2,5-Dicarbethoxy-3,4-diphenylcyclopentadienone (1). To a cooled solution of benzil (63.0 g, 300 mmol) and diethyl acetonedicarboxylate (72.6 g, 0.36 mol) in methanol (200 mL) was slowly added a solution of NaOH (12.0 g, 300 mmol) in methanol (12 g in 60 mL) with stirring. The mixture was warmed to room temperature and stirred overnight. The resultant yellow precipitate was filtered off and dried. H_2SO_4 was then added dropwise with stirring to a slurry of the yellow precipitate in acetic anhydride (350 mL) until all of the yellow precipitate had dissolved. An additional five drops of H_2SO_4 was then added to the solution. Finally, while the temperature of the solution was maintained below 80 °C, water was added dropwise to decompose excess acetic anhydride. The resultant orange precipitate was filtered off, air dried, and recrystallized from ligroine (100.5 g, 92%): mp 119−121 °C (lit. 120−121 °C).[25]

Diethyl 2,3-Diphenyl-1,4-benzenedicarboxylate (2). A solution of **1** (20 g, 55 mmol) and norbornadiene (24.48 g, 265 mmol) in toluene (75 mL) was refluxed for 5 h. The volume of solvent was reduced to 15 mL and methanol was added slowly to give a white precipitate. The white solid was filtered and recrystallized from methanol (17.3 g, 84%): mp 106−107 °C (lit. 110−112 °C).[25]

1,4-Bis(hydroxymethyl)-2,3-diphenylbenzene (3). A solution of **2** (17.3 g, 46 mmol) in anhydrous THF (175 mL) was added dropwise with stirring to a suspension of $LiAlH_4$ (7.89 g, 208 mmol) in anhydrous THF (350 mL) over a 30 min. period at 0 °C. The solution was stirred at room temperature for 1 h and then refluxed for an additional 5 h. The solution was then cooled in an ice bath, and with continuous stirring, water (8 mL) was added dropwise over 15 min. This was followed by 15% NaOH (24 mL) for another 15 min, and finally water (24 mL) was added over a 15 min period. The resulting mixture was stirred for 12 h and filtered, and then the product was recrystallized from aqueous methanol to give a white solid (11.61 g, 87%): mp 190−192°C; IR (KBr) 3076−3022 (aromatic C−H), 2910−2868 (aliphatic C−H), 3346−3349 cm^{-1} (OH); ^{1}H NMR (DMSO-d_6) δ 4.3 (d, 4 H), 5.0 (t, 2 H), 7.05 (m, 10 H), 7.67 (s, 2 H); ^{13}C NMR (DMSO-d_6) δ 61.15, 125.62, 126.13, 127.30, 129.61, 138.24, 138.66, 138.86; MS *m*/*e* (relative intensity (%)) 290 (100, M$^+$). Anal. Calcd for $C_{20}H_{18}O_2$: C, 82.73; H, 6.25. Found: C, 82.72; H, 6.03.

1,4-Bis(chloromethyl)-2,3-diphenylbenzene (4). A mixture of **3** (5 g, 17.2 mmol) and thionyl chloride (31 g, 260 mmol) was stirred overnight, and then the excess thionyl chloride was removed. The pale yellow product was then recrystallized from methanol (4.43 g, 78.9%): mp 97−99 °C; IR (KBr) 3057−3022 (aromatic C−H), 2966 cm^{-1} (aliphatic C−H); ^{1}H NMR ($CDCl_3$) δ 4.29 (s, 4 H), 7.0 (s, 10 H), 7.7 (s, 2 H); ^{13}C NMR ($CDCl_3$) δ 44.45, 126.61, 127.47, 129.37, 129.95, 135.95, 137.67, 141.63. MS *m*/*e* (relative intensity (%)) 327 (4.59, M$^+$), 255 (100). Anal. Calcd for $C_{20}H_{16}Cl_2$: C, 73.41; H, 4.93. Found: C, 73.57; H, 4.87.

Poly[(2,3-diphenyl-*p*-phenylene)(2-chloroethylene)] (5). A 3 mL aliquot of *t*-BuOK (1.0 M in THF) was added to a solution of **4** (1.0 g, 3.0 mmol) in THF (40 mL). The resulting solution was then stirred for 1 h at room temperature before being precipitated from methanol (200 mL). The precipitate was filtered off and air dried to give the chlorine precursor polymer (light yellow in color). The number and weight average molecular weights of the precursor polymer were 211 603 and 1 119 499 with an M_w/M_n ratio of 5.3, as determined by gel permeation chromatography. Anal. Calcd for $C_{20}H_{15}Cl$: C, 82.61; H, 5.20; Cl, 12.19. Found: 82.42; C, 5.29; H, Cl, 11.68 (Cl indicating a 5% conversion based on the chlorine content).

Poly[(2,3-diphenyl-*p*-phenylene)(2-chloroethylene)-phenylene(2-chloroethylene)]. *t*-BuOK (1.0 M) in THF (3 mL) was added to a solution containing **4** (0.5 g, 1.5 mmol) and 1,4-bis(chloromethylbenzene) (0.5 g, 1.5 mmol) in THF (45 mL). The resulting solution was then stirred for 1 h at room temperature before being precipitated from methanol (300 mL). The precipitate was filtered off and air dried to give the chlorine precursor copolymer of DP-PPV and PPV. Elemental

Scheme 1

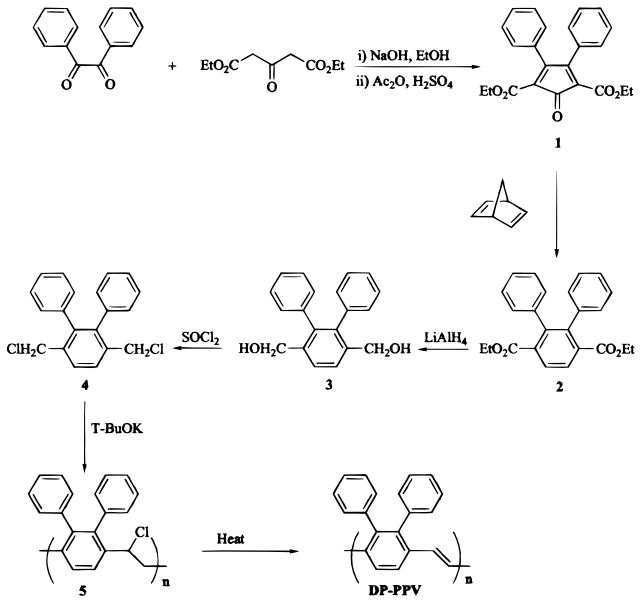

Table 1. Degree of Conversion of DP-PPV under Different Thermal Conditions

conditions	% C	% H	% Cl	total	deg of conv
as obtained (5)	82.42	5.29	11.68	99.39	5.0
230 °C/2 h	92.12	5.55	1.64	99.31	88.0
280 °C/2 h	93.68	5.55	0.50	99.73	97.0
DP-PPV (theory)	94.50	5.50	0	100.0	100.0

analysis showed 78.34% C, 5.27% H, and 14.40% Cl, corresponding to a precursor copolymer ratio of 4:1 DP-PPV to PPV (theory for a 4:1 ratio is 79.70% C, 5.44% H, and 14.86% Cl).

Results and Discussion

Synthesis. The monomer, 1,4-bis(chloromethyl)-2,3-diphenylbenzene was prepared in a four-step reaction according to Scheme 1. The condensation of benzil and diethyl acetonedicarboxylate in the presence of sodium hydroxide, followed by dehydration in acetic anhydride/sulfuric acid, gives **1**.[25] This undergoes the Diels−Alder reaction with norbornadiene to give **2**. The reduction of **2** with $LiAlH_4$ gives **3**, which is then converted to **4** with thionyl chloride. The monomer **4** is then polymerized by treatment with 1.1 equiv of potassium *tert*-butoxide (*t*-BuOK) to give the chlorine precursor polymer **5**. The precursor polymer **5** showed M_n and M_w of 1 119 499 and 211 603, respectively. Elemental analysis showed 82.42% carbon, 5.29% hydrogen, and 11.68% chlorine, indicating 5% conversion had occurred, based on the chlorine content. The polymerization of **4** with a 1.1 equiv of *t*-BuOK gives mostly soluble precursor polymer. Insoluble precursor polymers were obtained when 1.7 equiv of base was used. **5** is solvent cast onto a glass substrate and converted to DP-PPV, **6**, as a free-standing film (see Experimental Section) by thermal conversion at different conversion temperatures. The elemental analysis of DP-PPV converted at different temperatures showed different degrees of conversion based on the chlorine content, as shown in Table 1.

The Infrared spectra of **5** (top) and DP-PPV (bottom) converted at 230 °C are shown in Figure 1. They are very similar except for an additional peak at 968 cm^{-1} for DP-PPV, which is attributed to the out of plane deformation of trans C−H. A small amount of conversion of **5**, which was confirmed by elemental analysis, is evident in the IR with a vinylene C−H stretching

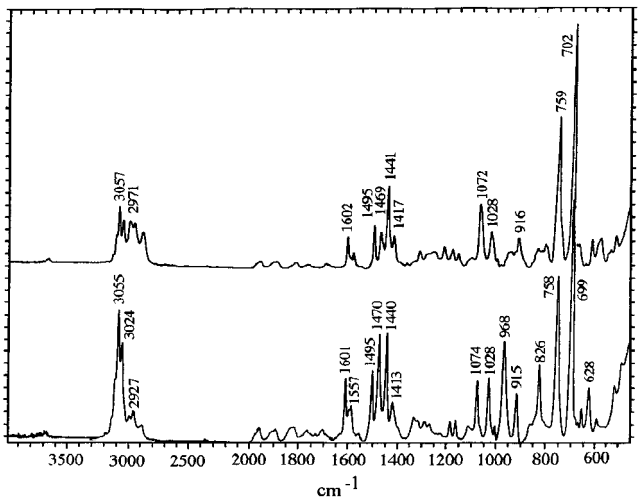

Figure 1. Infrared spectra of the polymer precursor **5** (top) and DP-PPV which was converted at 230 °C (bottom).

Table 2. Experimental Conditions Used for the Synthesis of Poly(DP-PPV-*co*-PPV)

amt of 1,4-bis(chloromethyl)-2,3-diphenylbenzene (mmol)	amt of 1,4-bis(chloromethy)benzene (mmol)	amt of *t*-BuOK (mmol)	THF (mL)	yield (%)	result
2.14	0.97	18	45	37	insoluble
1.5	1.5	18	45	53	insoluble
1.5	1.5	3.2	45	28	soluble

peak at 3057 cm^{-1}. This peak becomes very pronounced for DP-PPV at 3055 cm^{-1}.

We have also attempted to prepare poly(DP-PPV-*co*-PPV). Highly insoluble poly(DP-PPV-*co*-PPV) was obtained from copolymerization of **4** and 1, 4-bis(chloromethyl)benzene with a large excess of base (see Table 2).

We obtained a soluble precursor of poly(DP-PPV-*co*-PPV) with M_w and M_n of 818 780 and 31 148, respectively and a M_w/M_n ratio of 26 by using a 1:1 equivalent of base. It is interesting to note that a relatively narrow molecular weight distribution of 5.3 was obtained for DP-PPV while a broad molecular weight distribution of 26 was obtained for poly(DP-PPV-*co*-PPV) under similar polymerization conditions. Broad molecular weight distributions are not unknown, and the high M_w/M_n ratio is probably attributed to a distribution of polymeric chains of the copolymer. This may be due to the reaction conditions used for the polymerization procedure or possibly due to the different solubilities of monomers of PPV and DP-PPV. In addition, we did not optimize the molecular weight distributions for this copolymer. The observed elemental analysis data of 78.34% C, 5.27% H, and 14.40% Cl for the copolymer precursor corresponds well with the calculated values of 79.70% C, 5.44% H, and 14.86% Cl for the following formula:

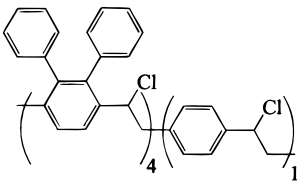

Optical Absorption and Photoluminescence of DP-PPV Converted at Different Temperatures. The conversion process of **5** in the form of thin films (400 Å) under nitrogen or high vacuum was investigated

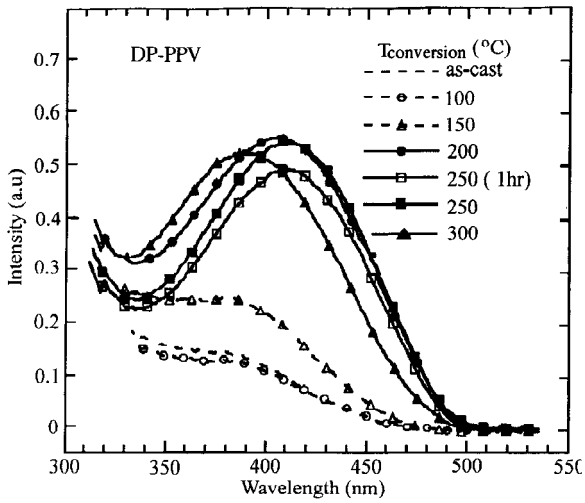

Figure 2. Absorption spectra of DP-PPV thermally converted at different conversion temperatures.

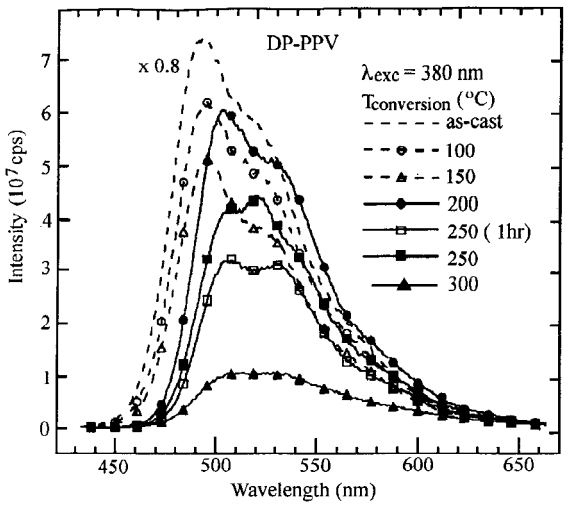

Figure 3. Emission spectra of DP-PPV thermally converted at different conversion temperatures.

by absorption and emission spectroscopy. The thermal conversion of (**5**) was performed at different temperatures. Figure 2 shows the absorption spectra of (**5**) for a set of samples converted at different temperatures between 100 and 300 °C for 2 h. The spectrum of the sample converted at 100 °C is almost identical to that of the precursor polymer. This indicates that thermal conversion does not easily occur at <100 °C, and that **5** is relatively robust. In fact, (**5**) can be stored under ambient conditions for more than 1 year without any detectable deterioration.

A weak absorption band at 390 nm emerges for the sample converted at 150 °C, which is indicative of thermal conversion. A relatively strong $\pi-\pi^*$ absorption band at 405 nm can be seen for the sample converted at 200 °C. The absorption band shows a red shift to 410 nm for the sample converted at 250 °C relative to the sample at 200 °C. The absorption band for the 300 °C sample shows a blue shift to about 385 nm and a reduction in intensity. These observations indicate that by increasing the temperature of thermal conversion from 150 to 250 °C, higher conjugation lengths and higher degrees of conversion can be achieved. At 300 °C, a reduction in intensity with a concurrent blue shift in the UV spectrum indicates thermal decomposition of the conjugated polymer. The λ_{max} at 405 nm and the band edge at 590 nm for DP-PPV are both blue shifted by approximately 30−40 nm with respect to PPV. This may be due to ineffective conjugation along the DP-PPV polymer backbone caused by steric hindrance of the bulky diphenyl groups. The bulky phenyl groups also result in low crystallinity for DP-PPV, which is reflected by the smooth $\pi-\pi^*$ absorption band without vibronic structure similar to the case of PPV with phenyl substituents.[26,27] The featureless spectrum is caused by disorder induced by the bulky phenyl substituents.

The steady state photoluminescent emission spectra for the same set of samples described above are shown in Figure 3. The PL spectra of the samples converted at 100 and 150 °C are essentially identical to that of the precursor polymer **5**, indicating the partially converted nature of these samples and the presence of identical emitting species. A red spectral shift is observed for the samples converted at 200 and 250 °C, which is indicative of their transformation to DP-PPV. The significant PL intensity drop for the 300 °C sample is attributed to thermal decomposition that forms defects which serve as the quenching sites. However,

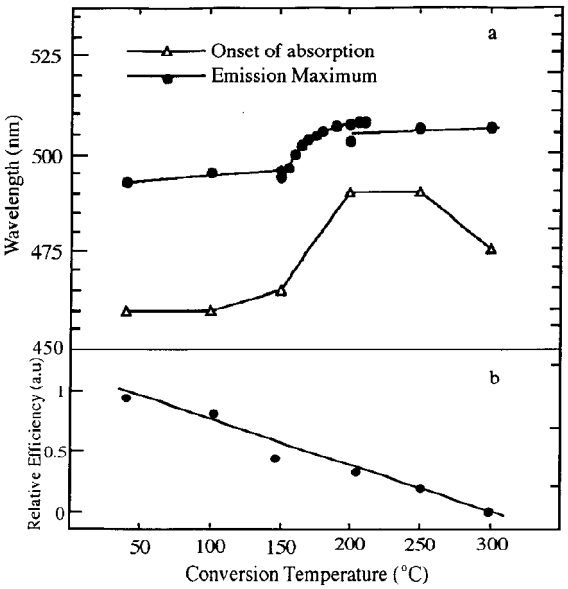

Figure 4. (a) Onset of the absorption and the main emission peak positions plotted as a function of the wavelength. A red shifts occur after the conversion temperature reaches 200 °C. (b) Plot of relative quantum efficiency of DP-PPV vs conversion temperature, which is decreasing with increasing conversion temperatures.

there is little spectral shift for the 300 °C sample, indicating that the emitting species remain the same as those samples converted at 200 and 250 °C.

In order to have a better understanding of the conversion process, we performed in situ PL measurements on a sample while it was being heated in the temperature range 150−200 ° C (Figure 4a). Shown in Figure 4a is the progression of the spectral shifts with respect to the conversion temperature. Both the band edge and the emission peak plots clearly show that 150 °C is the onset of thermal conversion and that 200−250 °C are the optimal conversion temperatures for achieving full conversion. A red shift in the emission spectra occurs continuously between 150 and 170 °C. Such a change was also observed in PPV where the red shift did not occur below 210 °C.[27] At 200 °C, both absorption and emission spectra of DP-PPV, have shifted to the red and stayed at these positions even at higher temperatures. The absorption spectrum's rising edge is at 490 nm, which is 30−40 nm blue-shifted relative to PPV. Steric hindrance by the phenyl sub-

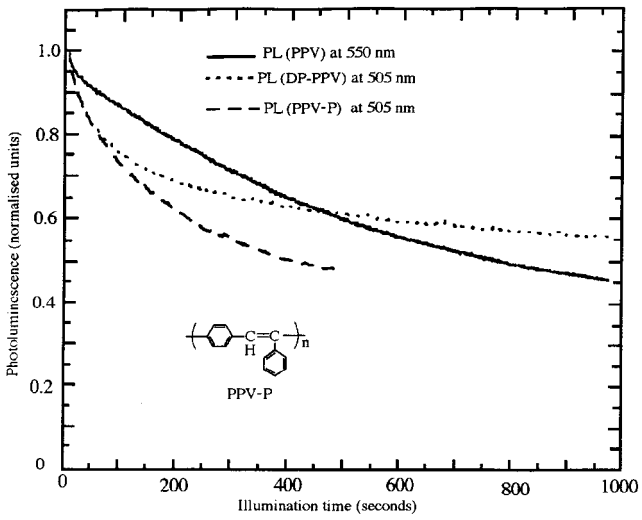

Figure 5. Comparison of the photoluminescence degradation with light exposure of DP-PPV, PPV, and PPV-P.

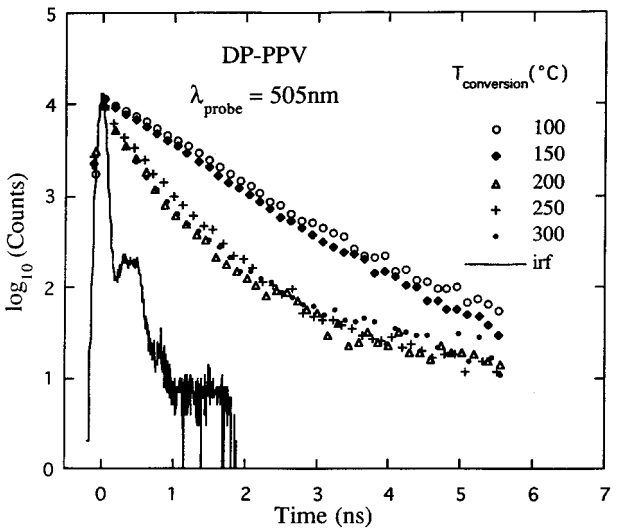

Figure 6. PL decay dynamics of DP-PPV probed at different temperatures. The single exponential decay when the conversion temperature is below 200 °C becomes more complex as the conversion temperature is above 200 °C.

stituents results in less effective conjugation as compared to PPV.[18] The red shift of the steady state spectra when the temperature reaches 150−170 °C infers that the conversion has a well-defined thermodynamic barrier. As the temperature increases from 200 °C, the relative quantum efficiency decreases with the conversion temperature but the spectral position remains unchanged (Figure 4b), which appears to indicate that the polymer becomes more crystalline as the temperature increases. We have reported previously that DP-PPV showed crystallinity according to X-ray diffraction studies.[30] However, electron diffraction studies of DP-PPV as a function of conversion temperature are needed to show if the decrease in luminescence that accompanies the increase in temperature is due to increased crystallinity. Photoluminescence efficiency decreases as a result of self-quenching due to a higher concentration of light-emitting centers. For the sample converted at 300 °C, the absorption spectrum exhibits a blue shift. When the conversion temperature reaches that high, decomposition and defect formation can take place. Carbonyl formation may lead to the breakdown of the polymer, which results in shorter conjugation lengths that have been reported for PPV.[28,29] This change in the chemistry of the polymer becomes predominant and is reflected by the slight blue shift of the absorption spectrum. Prolonged heating to 5 h under nitrogen at 250 °C did not produce any changes in the absorption or emission spectra of the sample. This indicates that the conversion of DP-PPV depends mainly on the temperature at which the sample is heated.

We examined the degradation of the PL as a function of the illumination time of DP-PPV, PPV, and PPV-P thin films (Figure 5). Time course PL studies indicate that initially, DP-PPV has an exponential like decay profile, as a function of the duration of light exposure under ambient conditions (light intensity is 1 mW/cm^2), unlike PPV, which appears almost linear in its initial decay profile. This difference in the initial decay profile for DP-PPV and PPV could imply different decay mechanisms. After 400 s, the decay profile of DP-PPV becomes similar to those reported for PPV and PPV-P (Figure 5). The PL decay can be prevented in DP-PPV by illuminating under a N_2 atmosphere, indicating photooxidation may be occurring, which is in agreement with that observed by others for PPV.[30−32]

Time-Resolved Emission Decay of DP-PPV Converted at Different Temperatures. We present in Figure 6 the time-resolved PL spectra probed at the emission peak maximum, 495 nm, for conversion temperatures below 150 °C and 505 nm for the conversion temperatures above 200 °C. Figure 6 shows that the PL decay lifetime (the time for the emission intensity to fall to 1/e of the initial PL) decreases from 1.17 to 1.02 ns as the conversion temperature increases from 100 to 150 °C. Faster decay in a more conjugated PPV has also been previously reported.[33] An increase in traps such as by carbonyl groups via photooxidation to account for the time-resolved emission spectra was discounted since we did not observe any peaks due to carbonyl groups in the infrared spectra of **5** and DP-PPV converted at 230 °C (Figure 1).

In the partially converted polymer, the single exponential decay points to one type of emitting chromophore and to a very localized exciton. Segments of oligo conjugated chains are separated from each other by the leaving group and other defects and can emit independently with little self-quenching. At 200−300 °C, the decay curves become even faster and the behavior becomes more complex. The decay lifetime for DP-PPV converted at 200−300 °C is about 0.32−0.42 ns. We know that the fully converted DP-PPV can be obtained at this temperature range. Nonradiative decay paths involving self-quenching by the interchain excitons[34] and/or exciplexes[35,36] is highly possible in the fully converted state due to the high concentration of the excited species. A shorter lifetime decay infers a larger mobility of the excitons.[37] The more rapid motion of the excitons accounts for the decrease in intensity of the steady-state emission as the conversion temperature increases. More excitons nonradiatively decay because of a larger probability of interaction with quenching sites. The nonsingle exponential behavior of the decay points to the existence of two processes for the light emission. The decays signal has a fast and a slow component. The fast component of the PL may be due to direct emission from the intrachain exciton, while the slow PL may be from interchain excitons re-formed to intrachain excitons.[34]

Photoconductivity for Free Standing Films of DP-PPV. The photoconductivity (PC) response and the subsequent relaxation for DP-PPV thin films (10 um) are presented in Figure 7. An electric field of about 105

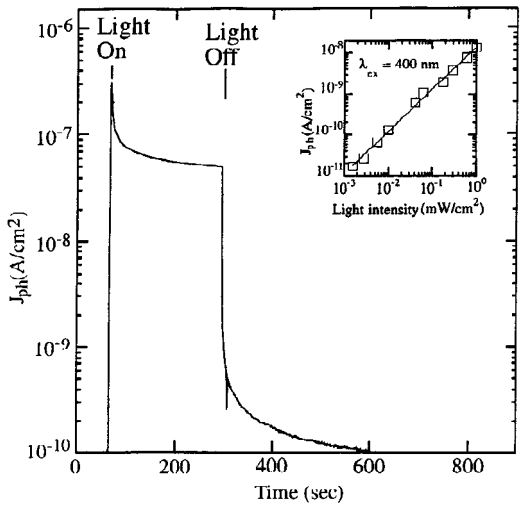

Figure 7. Buildup and decay of the steady state PC as a function of time. The applied field is 10^5 V/cm, and the monochromatic light is $\lambda_{exc} = 400$ nm. DP-PPV exhibits a strong PC response. The sublinear behavior of the photocurrent with the incident light is shown in the inset.

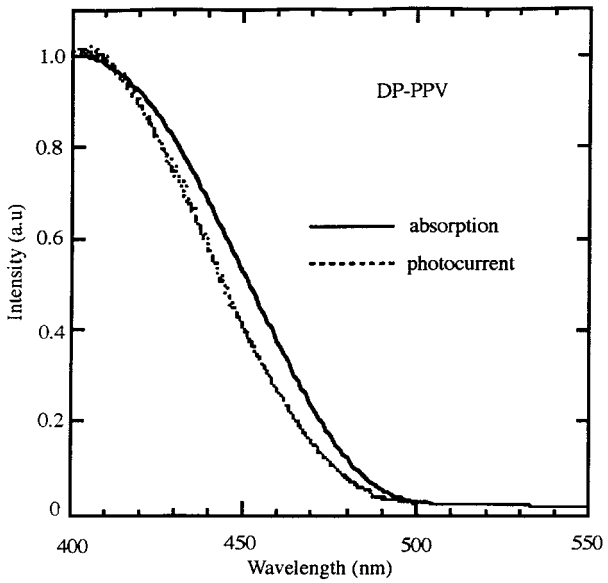

Figure 8. Optical absorption (full line) and the spectral response of the photocurrent (broken line) at an electric field of 10^5 V/cm.

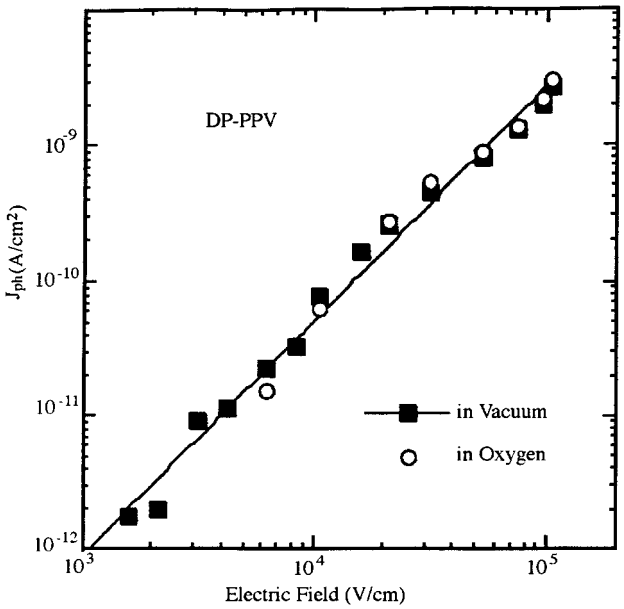

Figure 9. Electric field dependence of the photocurrent density at $\lambda_{exc} = 400$ nm and light intensity of about 0.3 mW/cm^2.

V/cm was applied across the device, and the sample was subjected to monochromatic light (400 nm) with light intensity of 0.3 mW/cm^2 for approximately 210 s. Under these conditions, the conductivity of the sample increased instantaneously by more than 3 orders of magnitude upon light exposure but decayed sharply to reach a steady-state after more than 50 s. This relaxation is an extrinsic effect and it was found to be more pronounced as the sample was exposed to air and to continuous illumination. The photocurrent relaxation upon illumination may be attributed to the relaxation of the electric field within the device caused probably by the space charge of trapped photocarriers or by other time dependent contact related effects commonly observed in these materials. Furthermore, when the light is off, the initial drop of the photocurrent is followed by a persistent current tail supporting the speculation of delayed emission of trapped carriers. The inset in Figure 7 shows the linear dependence of the photocurrent with the light intensity at $\lambda = 400$ nm and electric field of about 105 V/cm. The linear relation between the photocurrent and the light intensity suggests that the photocarrier generation rate is proportional to the number of photons absorbed and suggests that the density of photocarriers is low enough where bimolecular dynamics are not present. Figure 8 displays the spectral response of photoconductivity of DP-PPV together with its optical absorption spectrum. Each data point in the PC spectrum was measured 50 s after the light was turned on to allow the signal to reach equilibrium. Light intensity in the PC measurements were reduced by the use of neutral filters with an optical density totaling 2.0. The steady-state response of PC shows a threshold at about 490 nm, almost coincident with the onset of the $\pi-\pi^*$ interband transition in the tail of the absorption spectrum, and a peak at a position coinciding with the absorption maximum at 410 nm. The electric field dependence of the photocurrent for the free standing DP-PPV is shown in Figure 9. For this experiment the sample was kept in the cryostat and measurement was made under vacuum (10^{-2} Torr) and also in a dry oxygen atmosphere. The photocurrent was obtained by illumination at $\lambda = 400$ nm and at the intensity of 0.3 mW/cm^2. There was no significant difference in the photocurrent when testing conditions were changed from vacuum to oxygen. This indicates that the photogeneration is not influenced by molecular oxygen and if there is any oxidation it affects only the very top surface of DP-PPV. In general the photoconductivity of DP-PPV was found to be much lower than that of PPV. In an earlier publication[6] we found that ITO/PPV/Al devices, under similar conditions of illumination and electric field, can produce photocurrent densities in excess of 10^{-6} A/cm^2. Even higher photocurrent densities were detected in coplanar structures of PPV having gold or aluminum electrodes.[38] The low photocurrents and the absence of bimolecular recombination detected in DP-PPV devices may be related to higher density of traps present in this polymer or to a lower photocarrier generation efficiency with respect to PPV. More work needs to be done to clarify these issues further.

Electroluminescence of Single Layer and Bilayer DP-PPV LED Devices. For fabrication of the

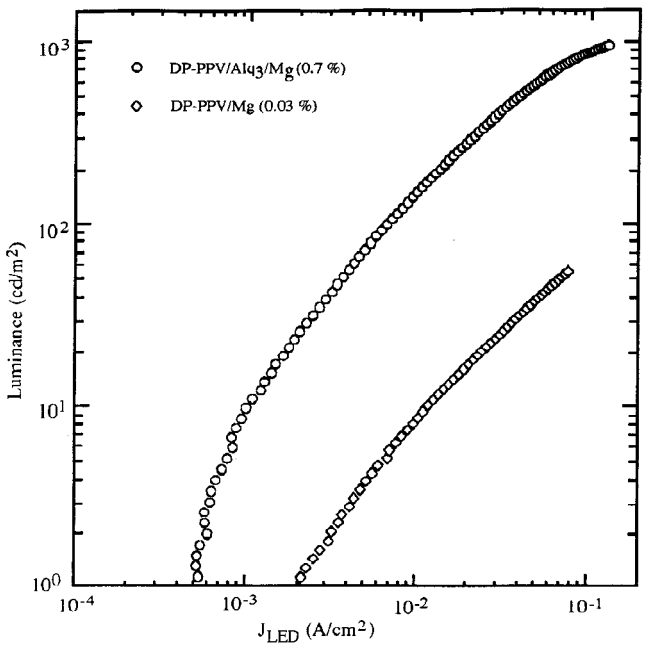

Figure 10. Luminance versus injection current density for single layer (ITO/DP-PPV/Mg) and bilayer (ITO/DP-PPV/Alq_3/Mg) devices. At 10 mA/cm^2 the corresponding external quantum efficiencies are 0.03% and 0.7% ph/el, respectively.

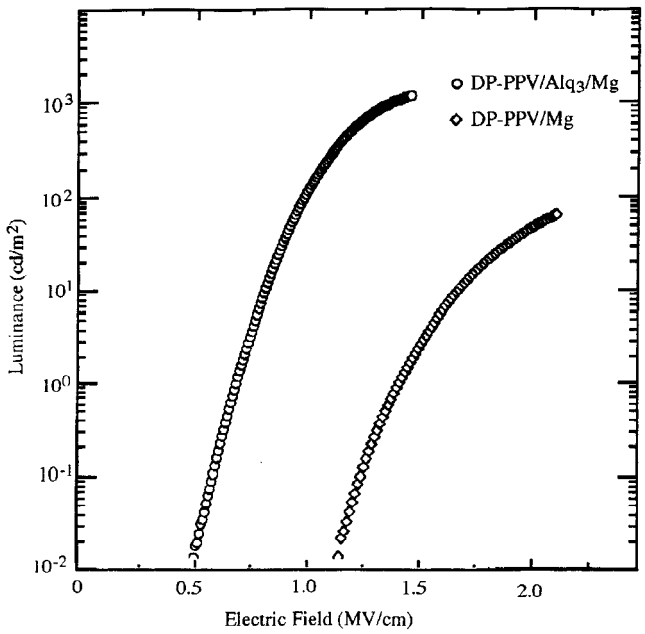

Figure 11. Luminance versus average applied electric field for single layer (ITO/DP-PPV/Mg) and bilayer (ITO/DP-PPV/Alq_3/Mg) devices.

DP-PPV LED devices, **5** was spin cast onto a indium−tin−oxide (ITO) coated glass substrate and converted to DP-PPV at 270 °C for 2 h under an inert atmosphere. Magnesium was then deposited on top of DP-PPV by vacuum evaporation to make the single layer ITO/DP-PPV/Mg LED device. The bilayer device consisted of an additional layer of tris(8-hydroxyquinoline)aluminum (Alq_3) located between DP-PPV and the Mg layer (ITO/DP-PPV/Alq_3/Mg). The EL spectra of the single layer and bilayer DP-PPV devices are similar, with the maximum at 500 nm. The EL spectra are virtually identical to the PL spectra converted at the same temperature except for a slight red shift. The similarities of the PL and EL spectra are in agreement with the spectra reported for other LEDs made from PPV and its derivatives, such as MEH-PPV and BCHA-PPV, which suggests that the same excitations are involved.[1,39,40]

Emissions of uniform green light were detected from the ITO/DP-PPV/Mg device with a turn-on voltage of 3 V. The turn-on voltage is one of the lowest observed for single layer conjugated polymer devices and is comparable to those reported for polymer/Ca devices.[40,41] The external EL quantum efficiency of ITO/DP-PPV/Mg is 0.04% ph/el (photons emitted per electrons injected). This is in contrast to the bilayer ITO/DP-PPV/Alq_3/Mg LED device, which shows a 20-fold increased quantum efficiency (0.7% ph/el).[42] This effect is illustrated in Figure 10, in which the luminance is plotted as a function of the injection current for the bilayer ITO/DP-PPV/Alq_3/Mg and the single layer ITO/DP-PPV/Mg devices. The improved efficiency for the bilayer device must be related to the improved injection of electrons from Mg to Alq_3 as well as the efficient electron transport within Alq_3. This layer also acts as a barrier to the holes and prevents them from reaching the Mg cathode. We have also plotted in Figure 11 the luminance as a function of the average applied electric field, which is defined as V/d, where d is the thickness of the DP-PPV layer and V is the applied voltage. The Alq_3 in the bilayer reduces the operating voltage considerably compared with the single layer without Alq_3. This is attributed to the improvement in electron injection and the improved balance of holes and electrons.[43]

Summary

High-quality DP-PPV films of 400 Å to 10 μm can be readily prepared by the chlorine precursor route. Absorption and emission measurements of samples converted at different temperatures shows the existence of a well-defined thermodynamic barrier at 150−170 °C in the conversion process. Below 150 °C, the polymer still exhibits the precursor properties, while above 170 °C, the polymer is fully converted to DP-PPV. Increasing the conversion temperature or converting for a longer peiod of time only leads to a morphology change that does not significantly affect the luminescence properties of the polymer. However, the thermal conversion is accompanied by the formation of carbonyl moieties within the polymer whose quenching effect on the PL becomes critical when the conversion temperature is as high as 300 °C. The photoconductivity of DP-PPV is 2−3 orders of magnitude less than PPV. A significant improvement in EL efficiency and a reduction in the turn-on voltage was observed for an ITO/DP-PPV/Mg device when a thin layer of Alq_3 was deposited between the cathode, Mg, and DP-PPV.

Acknowledgment. This work was supported in part by the National Science Foundation under grant No. DMR-9603019. W.C.W. was supported by the Center for Photoinduced Charge Transfer under NSF STC grant No. CHE-9120001. H.R. acknowledges the Graduate Fellowship from the African-American Institute. We thank Daniel Roitman for help with the EL studies, J. Vitale for his help in the PL study, and S. Atherton and M. R. Robinson for their help in the SPC study.

References and Notes

(1) Burroughes, J. H.; Bradley, D. D. C.; Brown, A. R.; Marks, R. N.; MaKay, K.; Friend, R. H.; Burn, P. L.; Holmes, A. B. *Nature* **1990**, *347*, 539.

(2) Hsieh, B. R. In *Polymeric Materials Encyclopedia*; Salamone, J. C., Ed.; CRC Press, Inc.: Boca Raton, FL, 1996; Vol. 9, p 6537 (see also references therein).
(3) Schott, M. In *Organic Conductors: Fundamentals and Applications*; Farges, (J.-P., Ed.; Marcel Dekker: New York, 1994; Vol. 12, pp 539−646.
(4) Horowitz, G. *Adv. Mater.* **1990**, *2*, 287−292.
(5) (a) Sariciftci, N. S.; Braun, D.; Zhang, C.; Srdanov, V. I.; Heeger, A. J.; Stucky, G.; Wudl, F. *Appl. Phys. Lett.* **1993**, *62*, 585. (b) Sariciftci, N. S.; Smilowitz, L.; Heeger, A. J.; Wudl, R. *Synth. Met.* **1993**, *59*, 333.
(6) Antoniadis, H.; Hsieh, B. R.; Abkowitz, M. A.; Jenekhe, S. A.; Stolka, M. *Synth. Met.* **1994**, *62*, 265−271.
(7) (a) Hsieh, B. R.; Antoniadis, H.; Abkowitz, M. A.; Stolka, M. *Polym. Prepr. (Am. Chem. SOc., Div. Polym. Chem.)* **1992**, *33* (2), 414−415. (b) Antoniadis, H.; Hsieh, B. R.; Abkowitz, M. A.; Jenekhe, S. A.; Stolka, M. *Mol. Cryst. Liq. Cryst.* **1994**, *256*, 381. (c) Antoniadis, H.; Abkowitz, M. A.; Hsieh, B. R. *Appl. Phys. Lett.* **1994**, *65*, 2030. (d) Antoniadis, H.; Abkowitz, M. A.; Hsieh, B. R.; Jenekhe S. A.; Stolka, M. *Mater. Res. Soc. Symp. Proc.* **1994**, *328*, 377. (e) Abkowitz, M. A.; Antoniadis, H.; Facci, J. S.; Hsieh, B. R.; Stolka, M. *Synth. Met.* **1994**, *67*, 187−191.
(8) (a) Koezuka, H.; Tsumura, A.; Fuchigami, H.; Kuramoto, K. *Appl. Phys. Lett.* **1993**, *62*, 1794−1796. (b) Fuchigami, H.; Tsumura, A.; Koezuka, H. *Appl. Phys. Lett.* **1993**, *63*, 1372−1374.
(9) Garnier, F.; Hajlaoui, R.; Yassar, A.; Srivastava, P. *Science* **1994**, *265*, 1684.
(10) Dodabalapur, A.; Torsi, L.; Katz, H. E., *Science* **1995**, *268*, 270.
(11) Yang, Y.; Heeger, A. J. *Nature* **1994**, *372*, 344.
(12) (a) Bradley, D. D. C. *Adv. Mater.* **1994**, *4*, 756. (b) Baigent, D. R.; Greenham, N. C.; Gruner, J.; Marks, R. N.; Friend, R. H.; Moratti, S. C.; Holmes, A. B., *Synth. Met.* **1994**, *67*, 3. (c) Cacialli, F.; Friend, R. H.; Moratti, S. C.; Holmes, A. B. *Synth. Met.* **1994**, *67*, 157.
(13) Pei, Q.; Yu. G.; Zhang, C.; Yang, Y.; Heeger, A. J. *Science* **1995**, *269*, 1086.
(14) MacDiarmid, A. D.; Wang, H. L.; Huang, F.; Avlyanov, J. K.; Wang, P. C.; Swager, T. M.; Huang, Z.; Epstein, A. J.; Wang, Y.; Gebler, D. D.; Shashidhar, R.; Calvert, J. M.; Crawford, R. J.; Vargo, T. G.; Whitesides, G. M., Hsieh, B. R. *MRS Proc.* **1996**.
(15) Burn, P. L.; Kraft, A.; Baigent, D. R.; Bradley, D. D. C.; Brown, A. R.; Friend, R. H.; Gymer, R. W.; Holmes, A. B.; Jackson, R. W. *J. Am. Chem. Soc.* **1993**, *115*, 10117−10124.
(16) Hsieh, B. R. *Polym. Mater. Sci. Eng.* **1992**, *67*, 252.
(17) Hsieh, B. R.; et al. U.S. Patent Application.
(18) Hsieh, B. R.; Antoniadis, H.; Bland, D. C.; Feld, W. A. *Adv. Mater.* **1995**, *7*, 36−39.
(19) Hsieh, B. R.; Razafitrimo, H.; Gao, Y.; Feld, W. A. *Polym. Mater. Sci. Eng.* **1995**, *73*, 557−558.
(20) Hsieh, B. R.; Razafitrimo, H.; Gao, Y.; Feld, W. A. *Polym. Prepr. (Am. Chem. Soc., Div. Polym. Chem.)* **1995**, *36* (2), 85−86.
(21) Son, S.; Dodabalapur, A.; Lovinger, A. J.; Galvin, M. E. *Science* **1995**, *269*, 376.
(22) Fou, A. C.; Onitsuka, O.; Ferreira, M.; Rubner, M. F.; Hsieh, B. R. *J. Appl. Phys.*, submitted for publication.
(23) Onitsuka, O.; Fou, A. C.; Ferreira, M.; Hsieh, B. R.; Rubner, M. F.; Submitted for publication to *Science.*
(24) Hsieh, B. R.; et. al. *Proc. IS&T*, in press.
(25) (a) Reinhardt, B. A. Carboethoxy-Substituted Polyphenylenes M.S. Thesis, WSU, 1971. (b) Harris, W. H.; Reinhardt, B. A. *Polym. Prepr. (Am. Chem. Soc., Div. Polym. Chem.)* **1974**, *15* (1), 691−695.
(26) Gaiberger, M.; Bässler, H. *Phys. Rev. B* **1991**, *44*, 8643.
(27) Bradley, D. D. C.; Friend, R. H. *Synth. Met.* **1987**, *17*, 651.
(28) Papadimitrakopoulos, F.; Yan, M.; Rothberg, L. J.; Katz, H. E.; Chandross, E. A.; Galvin, M. E. *Mol. Cryst. Liq. Cryst.* **1994**, *256*, 663.
(29) Papadimitrakopoulos, F.; Konstanidis, K.; Miller, T. M.; Opila, R.; Chandross, E. A.; Galvin, M. E. *Chem. Mater.* **1994**, *6*, 1563.
(30) Hsieh, B. R.; Feld, W. A. *Polym. Prepr. (Am. Chem. Soc., Div. Polym. Chem.)* **1993**, *34* (2), 410.
(31) Cumpston, B. H.; Jensen, K. F. *Synth. Met.* **1995**, *73*, 195.
(32) Sutherland, D. G. J.; Carlisle, J. A.; Elliker, P.; Fox, G.; Hagler, T. W.; Jimenez, I.; Lee, H. W. H.; Pakbaz, K.; Terminello, L. J.; Williams, S. C.; Himpsel, F. J.; Shuh, D. K.; Tong, W. M.; Callcot, T. A.; Ederer, D. L *Appl. Phys. Lett.* **1996**.
(33) Samuel, I. D. W.; Crystall, B.; Rumbles, G.; Burns, P. L.; Holmes. A. B.; Friend, R. H. *Synth. Met.* **1993**, *54*, 281.
(34) Yan, M.; Rothberg, L.; Papadimitrakopoulos, F.; Galvin, M. E.; Miller, T. M. *Phys. Rev. Lett.* **1994**, *73*, 744.
(35) Jenekhe, S. A.; Osaheni, J. A. *Science* **1994**, *265*, 765.
(36) Gilbert, A.; Baggot, J. *Essentials of molecular photochemistry*; CRC Press: Boca Raton, FL, 1991.
(37) Pichler, K.; Halliday, D. A.; Bradley, D. D. C.; Burns, P. L.; Friend R. H.; Holmes, A. B. *J. Phys. Condens. Matter* **1993**, *5*, 7155.
(38) Antoniadis, H.; Rothberg, L. J.; Papadimitrakopoulos, F. Yan, M.; Galvin, M. E.; Abkowitz, M. A. *Phys. Rev. B* **1994**, *50*, 14911.
(39) Parker, I. D. *J. Appl. Phys.* **1994**, *75*, 1656.
(40) Zhang, C.; Hoger, S.; Pakbaz, K.; Wudl, F.; Heeger, A. J. *J. Electron. Mater.* **1993**, *22*, 413.
(41) Braun, D.; Heeger, A. J. *Appl. Phys. Lett.* **1991**, *58*, 1982.
(42) Wu, C. C.; Chun, J. K. M.; Burrows, P. E.; Sturm, J. C.; Thompson, M. E.; Forrest, S. R.; Register, R. A. *Appl. Phys. Lett.* **1995**, *66*, 653.
(43) Littman, J.; Martic, P *J. Appl. Phys.* **1992**, *72*, 1957.

MA971025U